Computed tomography segmental calcium score (SCS) to predict stenosis severity of calcified coronary lesions.

Pugliese, F; Hunink, MG; Meijboom, WB; Gruszczynsnka, K; Rengo, M; Zou, L; Baron, I; Dijkshoorn, ML; Krestin, GP; de Feyter, PJ

For additional information about this publication click this link.
http://qmro.qmul.ac.uk/xmlui/handle/123456789/12342

International Journal of Cardiovascular Imaging

Computed tomography segmental calcium score (SCS) to predict stenosis severity of calcified coronary lesions

--Manuscript Draft--

Abstract:	**Purpose** To estimate the probability of ≥50% coronary stenoses based on computed tomography (CT) segmental calcium score (SCS) and clinical factors. **Materials and Methods** The Institutional Review Board approved the study. A training sample of 201 patients underwent CT calcium scoring and conventional coronary angiography (CCA). All patients consented to undergo CT before CCA after being informed of the additional radiation dose. SCS and calcification morphology were assessed in individual coronary segments. We explored the predictive value of patient's symptoms, clinical history, SCS and calcification morphology. We developed a prediction model in the training sample based on these variables then tested it in an independent test sample. **Results** The odds ratio (OR) for ≥50% coronary stenosis was 1.8-fold greater (p = 0.006) in

patients with typical chest pain, 2-fold (p = 0.014) greater in patients with acute coronary syndromes, 2-fold greater (p <0.001) in patients with prior myocardial infarction. Spotty calcifications had an OR for ≥50% stenosis 2.3-fold (p <0.001) greater than the absence of calcifications, wide calcifications 2.7-fold (p <0.001) greater, diffuse calcifications 4.6-fold (p <0.001) greater. In middle segments, each unit of SCS had an OR 1.2-fold (p <0.001) greater than in distal segments; in proximal segments the OR was 1.1-fold greater (p = 0.021). The ROC curve area of the prediction model was 0.795 (0.95 confidence interval: 0.602-0.843). Validation in a test sample of 201 independent patients showed consistent diagnostic performance.

Conclusion
In conjunction with calcification morphology, anatomical location, patient's symptoms and clinical history, SCS can be helpful to estimate the probability of ≥50% coronary stenosis.

| Response to Reviewers: | COMMENTS FOR THE AUTHOR
* and Point-to-point responses *

Reviewer #1: The authors have conducted a detailed analysis of a novel evaluation of non-contrast computed tomographic coronary calcium. They use their novel segmental coronary calcium score in a cross-sectional study in a prediction model for odds ratio of stenosis.

Comment #1: The concept is not entirely novel as there have been many groups that have
reported a variety of methods to go beyond the Agatston-Janowitz calcium score. The challenge is that so many work stations have the AJ score already in place, and there is an abundance of literature behind the AJ score already. So there is a heavy inertia to overcome which would require something really useful.

* We agree with this reviewer that the Agatston score is the most widely used clinically, which is probably backed by vast prognostic data obtained decades ago. We used here however a segmental Agatston score, to evaluate if the "local" quantity of calcification can help interpret coronary CTA, when coronary CTA interpretation is limited by a visual effect known as the "blooming effect". *

Comment #2: While the methods are detailed and interesting and the score does predict stenosis, ultimately a symptomatic patient will just get a CTA to evaluate non-calcified and calcified plaque.

* We fully agree with this reviewer. However the interpretation of coronary CTA in heavily calcified vessels may be challenging. We hypothesized that segmental calcium score may be an aid to coronary CTA interpretation when the latter is difficult to interpret due to bulky calcifications. We are not proposing to replace coronary CTA with segmental calcium score. *

Comment #3: The manuscript is lengthy and could be condensed in the discussion.
In spite of these conceptual limitations, the study is interesting with a sound design and analysis.

* We have shortened the Discussion and removed the Appendix from the manuscript, as recommended by this reviewer and by the Editors. *

Reviewer #3: This is an attempt to build a multivariable model to predict significant stenosis in particular coronary artery segments using segmental calcium score and a variety of clinical parameters. It is exemplary in its use of a large dataset, appropriately split into training and test sets, and in the methods used to construct the model, for example, the use of GEE to derive the prediction model, given that the variables |

selected likely have a high degree of interdependence. I also liked the fact that the gold standard was catheter angiography rather than CCTA.

Comment #1: I do have doubts as to the clinical utility of this approach, however. In our practice, and in the practice at other institutions with which I am familiar, calcium scoring is simply not used in the acute setting. In an intermediate-risk acute patient, CCTA with calcium scoring may be employed, but in this situation, any patient with a difficult-to-quantitate heavily calcified lesion is going catheter angiography, and this prediction model would not be helpful here. In non-acute patients getting calcium scoring for risk assessment, again it is hard to imagine how this model might be used, perhaps only in very select circumstances to direct additional testing in intermediate-risk patients who are flagged as "high-risk" by use of this model. Regardless, I think this paper should be published for two reasons. First, I think it is a model paper demonstrating how prediction models of this type should be constructed and evaluated. I have seen too many papers of this type over the years with severe methodologic flaws, so it's nice to see one properly done. Second, I enjoyed the authors discussion and in particular, the "future developments" section. The authors' thoughts here will be very helpful providing ideas for future work.

* We thank this reviewer for his/her kind and constructive comments.
- 1. We have mentioned and referenced in our Discussion the ability to obtain calcium score from coronary CTA, by using either subtraction approaches or dual-energy protocols, without performing an additional pre-contrast scan. This could in principle overcome the issue of patients not routinely receiving non-contrast scans prior to coronary CTA, as mentioned by the reviewer.
- 2. In stable, intermediate risk patients, we agree that some practices may prefer to refer to invasive angiography cases where calcified lesions challenge the interpretation of coronary CTA. However, this is likely to lead to a number of unnecessary invasive procedures. Once the coronary CTA has been acquired, we should try to maximize its diagnostic yield both to diagnose and rule-out clinically relevant lesions. Strategies to reduce falsely positive findings on coronary CTA should be sought. Whilst we have discussed new approaches (FFRCT, perfusion imaging etc.) in our Discussion, we describe in our manuscript an approach that uses existing non-contrast calcium score data (which are still part of the standard clinical protocol at most institutions) and clinical data, without additional time-intensive post-processing (e.g. FFRCT) and without additional imaging, radiation, contrast and/or pharmacological stress (e.g. perfusion imaging). *

Computed tomography segmental calcium score (SCS) to predict stenosis severity of calcified coronary lesions

Manuscript type: Original Research (Word count: 3510; Images: 5; Tables: 5).

Abbreviations

CT = computed tomography

SCS = segmental calcium score

CCTA = coronary computed tomography angiography

CCA = conventional coronary angiography

OR = odds ratio

CI = confidence interval

ROC = receiver operating characteristic

AUC = area under the curve

EBT = electron-beam tomography

bpm = beats per minute

ECG = electrocardiogram

AHA = American Heart Association

QCA = quantitative coronary angiography

RCA = right coronary artery

LAD = left anterior descending coronary artery

LCx = left circumflex artery

LM = left main trunk

Abstract

Purpose

To estimate the probability of ≥50% coronary stenoses based on computed tomography (CT) segmental calcium score (SCS) and clinical factors.

Materials and Methods

The Institutional Review Board approved the study. A training sample of 201 patients underwent CT calcium scoring and conventional coronary angiography (CCA). All patients consented to undergo CT before CCA after being informed of the additional radiation dose. SCS and calcification morphology were assessed in individual coronary segments. We explored the predictive value of patient's symptoms, clinical history, SCS and calcification morphology. We developed a prediction model in the training sample based on these variables then tested it in an independent test sample.

Results

The odds ratio (OR) for ≥50% coronary stenosis was 1.8-fold greater (p = 0.006) in patients with typical chest pain, 2-fold (p = 0.014) greater in patients with acute coronary syndromes, 2-fold greater (p <0.001) in patients with prior myocardial infarction. Spotty calcifications had an OR for ≥50% stenosis 2.3-fold (p <0.001) greater than the absence of calcifications, wide calcifications 2.7-fold (p <0.001) greater, diffuse calcifications 4.6-fold (p <0.001) greater. In middle segments, each unit of SCS had an OR 1.2-fold (p <0.001) greater than in distal segments; in proximal segments the OR was 1.1-fold greater (p = 0.021). The ROC curve area of the prediction model was 0.795 (0.95 confidence interval: 0.602-0.843). Validation in a test sample of 201 independent patients showed consistent diagnostic performance.

Conclusion

In conjunction with calcification morphology, anatomical location, patient's symptoms and clinical history, SCS can be helpful to estimate the probability of ≥50% coronary stenosis.

Introduction

The total amount of coronary artery calcification quantified by electron beam tomography or more recently by multidetector computed tomography (CT) correlates with the probability of angiographically significant (≥50% diameter reduction) stenosis at the patient level (1-4). A calcium score of 0 indicates a low probability of ≥50% coronary stenosis (1). A calcium score ≥400 indicates a relatively high probability of ≥50% coronary stenosis in patients ≥50 years old anywhere in the coronary tree. This information is not site-specific. The total calcium score does not provide information regarding the probability of stenosis at the level of a specific coronary segment or lesion. Moreover, the relationship between intermediate values of calcium score (e.g., between 1 and 399) and associated stenosis is weak. Contrast-enhanced coronary CT angiography (CCTA) can overcome the known diagnostic limitations of calcium score. Unfortunately though, bulky calcifications may hinder the visualization of the coronary lumen at CCTA ("blooming effect"), thus the evaluation of stenosis severity in calcified vessels can be challenging.

The purpose of this study was to develop an algorithm for estimating the probability ≥50% coronary stenoses based on CT segmental calcium score (SCS) and clinical factors. The algorithm consists of a multivariable prediction model that includes the SCS measured in a given coronary segment, the patient's symptoms and clinical history to calculate the probability of ≥50% coronary artery stenosis in the same coronary segment.

Materials and Methods

Patients

The Institutional Review Board approved the study protocol. All patients consented to undergo CT before CCA after being informed of the additional radiation dose. They also consented on the use of their data for retrospective research.

During a 24-month period, 402 patients with stable or acute chest pain were recruited to an ongoing study (5) comparing 64-detector row CCTA with conventional coronary angiography (CCA). Patients in sinus heart rhythm, able to hold their breath for 15 seconds and without previous coronary revascularization were included. Impaired renal function (serum creatinine >120 μmol/L) and known contrast allergy were exclusion criteria.

Preparation and coronary calcium scans

Patients with heart rates >65 beats per minute (bpm) received 100 mg metoprolol orally 1 hour before the scan. Scans were performed with a 64-detector row CT scanner with a gantry rotation time of 330 ms, a temporal resolution of 165 ms and a spatial resolution of 0.4 mm^3 (Somatom Sensation 64; Siemens, Forchheim, Erlangen, Germany).

The non-enhanced coronary calcium scans were acquired with a standard spiral low-dose protocol using ECG-gating. Scan parameters were as follows: 32*2 slices per rotation with z-flying focal spot technology, providing 64 slices/rotation; 0.6 mm individual detector width, 330 ms rotation time, 3.8 mm/rotation table feed, 19.2mm beam width, 11.5mm/s table speed, 120 kV tube voltage, 150 mAs tube current, with activated prospective x-ray tube modulation. Overlapping slices were reconstructed at 65% of the R-R interval (retrospective ECG-gating) using B35f convolution kernel. Reconstructed slice thickness was 3.0 mm with an increment of 1.5 mm. The radiation exposure, estimated using dedicated software (ImPACT, version 0.99x, St. George's Hospital, Tooting, London, United Kingdom), was 1.4 mSv in men and 1.8 mSv in women.

Computed tomography coronary angiography (CCTA) scans

For the contrast-enhanced CCTA studies, 80 ml of contrast agent (iomeprol; Iomeron, 400 mg/ml; Bracco, Milan, Italy) were injected intravenously into an antecubital vein. The injection rate was 5

ml/s. A bolus-tracking technique was used to time the scan (5-7). Scan parameters were identical to those used for coronary calcium scanning except for a tube current of 900mAs. Datasets were reconstructed using retrospective ECG gating and a mono-segmental reconstruction algorithm (5-7). Overlapping slices were reconstructed at 65% of the R-R interval (retrospective ECG-gating) using a medium-smooth convolution kernel. Reconstructed slice thickness was 0.75 mm with an increment of 0.4 mm. The estimated radiation exposure was 14.2 mSv in men and 18.4 mSv in women, in keeping with estimated X-ray radiation exposure values reported using similar CT technology (64-slice) and scan protocol (retrospective ECG-gating) (8).

Conventional coronary angiography (CCA)

CT and CCA were carried out within a time interval of 1 week. A single observer (>10-year experience) identified coronary segments on CCA following a 17-segment modified American Heart Association (AHA) classification model (9). Coronary stenoses with diameter reduction ≥50% were identified using validated quantitative coronary angiography (QCA) software (CAAS II®, Pie Medical, Maastricht, the Netherlands).

Analysis of segmental calcium score (SCS) and calcification morphology

CT datasets were analyzed using an off-line workstation (syngo MultiModality Workplace VE25A, Siemens, Erlangen, Germany). Dedicated software (syngo Calcium Scoring VE31H, Siemens, Germany) was used for measuring calcium score in non-enhanced scans (10). One experienced observer, unaware of the CCA results, measured segmental calcium scores (SCS) in individual coronary segments using a standard technique based on seed points and a region-growing algorithm. Results were expressed using the Agatston (11), volume (12) and mass (13) scores. The analysis is described in detail in Figure 1 and Figure 2. As shown in Figure 3, calcification morphology in each segment was classified as spotty, wide or diffuse based on the width and length of the calcification in relation to the coronary segment diameter, following a validated classification model previously described by Kajinami et al. (14) (Table 1). In the event of multiple calcifications with different morphology within the same segment, the segment was classified as the calcification with the largest size.

In this study the outcome of interest was ≥50% diameter stenosis as demonstrated by the gold standard invasive CCA. CCTA was used exclusively for the anatomical classification of coronary segments, but not for grading lesion severity. The evaluation of the diagnostic performance of CCTA in the identification of coronary stenosis compared to CCA was reported previously (ref. blinded for review) and was beyond the purpose of this study.

Statistical analysis

Statistical analysis was performed using commercially available software (IBM SPSS, version 20, Chicago, IL, and STATA/SE 10.0, College Station, TX). Quantitative variables were expressed as means (standard deviations) and categorical variables were expressed as frequencies or percentages. The definitions of variables such as symptoms and risk factors are given in Table 2. The level of significance was chosen at a p-value <0.05.

Data from 402 patients were split into two equal-sized datasets. One dataset containing 201 patients was used to derive the multivariable prediction model (training set) and the remaining 201 patients were used to validate the prediction model (test set). Baseline characteristics were compared between two sets (Table 2). Continuous variables were tested using Mann-Whitney U test and categorical variables were compared with the chi-squared statistic.

In the training set, we identified highly correlated variables, explored the predictive value of the variables and derived a multivariable prediction model. There was high correlation between the Agatston and the volume scores (Pearson r = 0.990; p <0.001), the Agatston and the mass scores (r = 0.995; p <0.001) and the volume and the mass scores (r = 0.989; p <0.001). We used the Agatston score for further analyses because it has been extensively validated in clinical practice (1-4, 11). In the training set, we determined the frequency of the outcome of interest i.e. ≥50% stenoses at the segment level according to ranges of SCS and calcification morphology. Stenoses with a diameter narrowing ≥50% at CCA were defined as the reference standard to define positive cases. This is in accordance to the definition of 'significant' stenosis most widely used in cardiac

CT literature. The natural log transforms of (SCS + 1) were used because SCS showed a skewed distribution.

We performed univariable analyses to evaluate the significance of SCS in each segment, calcification morphology, segment location (proximal, middle, and distal/side branches, as previously described (15)), major coronary vessel (RCA, LAD, LCx, LM), age, gender, patient's symptoms (typical chest pain/atypical chest pain/acute coronary syndrome), risk factors (obesity, hypertension, smoking, diabetes mellitus, hypercholesterolemia, family history of premature coronary artery disease) and clinical history (prior myocardial infarction) for the prediction of $\geq 50\%$ stenosis. Variables with a p-value <0.10 in the univariable analyses were entered in the multivariable model. Interaction terms were explored between morphology and SCS, location and SCS, location and morphology, vessel and SCS, and vessel and morphology. The final multivariable model included all variables with a p-value <0.05 and variables with a p-value <0.10 that were considered to be important based on clinical judgment and internal consistency of the model. Odds ratios (OR) and robust 95% confidence intervals (CI) are reported.

Generalized estimating equations (GEE) with binomial family, logit link function, exchangeable correlation matrix, and robust –sandwich– standard errors was applied to drive the prediction model on the training set. This took into account of the clustering feature that each patient had multiple segments measured. Receiver-operating characteristic (ROC) curve with area under the curve (AUC) was used to access the performance of the prediction model. The derived prediction model was then validated by the test set.

Results

Baseline characteristics and angiographic findings (Table 2)

In the training set, 126/201 (62.7%) patients had at least one ≥50% stenosis (Table 2). A total of 3001 coronary segments were visualized angiographically. Of these, 136/3001 (4.5%) were localized distally to occluded coronary segments and supplied by collateral pathways thus were excluded from the analysis. There remained 2865 coronary segments, of which 282/2865 (9.8%) harboured ≥50% stenoses. Among the lesions associated with ≥50% stenosis, 89/282 (31.6%) were in the RCA, 110/282 (39%) in the LAD, 79/282 (29%) in the LCx, and 4/282 (1.4%) in the LM (p <0.001).

Total calcium score and frequency of stenosis anywhere in the coronary tree (patient level)

In the training set, the median (interquartile range) total calcium score at patient level was 198.10 (10.65 - 557.40). The frequency of at least one coronary stenosis at the patient level increased proportionally with increasing total calcium score (p-value <0.001). In patients with a total Agatston calcium score in the range 0-10, 5/50 (10%) patients had at least one significant stenosis. In patients with a total calcium score in the range 11-100, 20/32 (62.5%) patients had at least one significant stenosis. In patients with a total calcium score in the range 101-400, 45/59 (76.3%) patients had at least one significant stenosis. In patients with a total calcium score >400, 56/60 (93.3%) had at least one significant stenosis. The AUCs of total Agatston score for the detection of ≥50% coronary stenosis at the patient level was 0.851 (CI: 0.681-0.900). The odds ratio (OR) for ≥50% stenosis anywhere in the coronary tree (patient level) was approximately 1.9-fold greater (p <0.001) for each unit of natural log of total calcium score (OR=1.908; CI: 1.664-2.375).

Segmental calcium score (SCS)

In the training set, the range in SCS was 0-1370. The median (interquartile range) was 0 (0 - 6.65). There were 1735/2865 (60.6%) segments which did not show any detectable calcification (SCS = 0). Of these, 68/1735 (3.9%) harboured a ≥50% stenosis.

Calcification morphology

In the training set, there were 431/2865 (15%) spotty calcifications, 325/2865 (11.3%) wide calcifications, and 374/2875 (13.1%) diffuse calcifications.

Frequency of significant stenoses

The frequency of coronary stenosis increased proportionally with increasing SCS (Figure 4, left column), and from spotty, to wide, to diffuse morphology (all p-values <0.01). The frequency of significant stenoses associated with SCS and morphology in men and women according to age is given in Table 3. The AUCs for the detection of ≥50% coronary stenosis were 0.739 (CI: 0.706-0.771) for SCS, and 0.738 (CI: 0.706-0.771) for calcification morphology (Figure 4, right column).

Univariable analysis (Table 4)

The odds ratio (OR) for ≥50% stenosis was approximately 1.7-fold (p = 0.005) greater for patients with typical chest pain and 1.6-fold (p = 0.023) greater for patients with unstable angina or non-ST elevation myocardial infarction (acute coronary syndrome). For patients with dyslipidemia, the OR was increased 2.6-fold (p <0.001), and for patients with a prior myocardial infarction the OR was increased 2.5-fold (p<0.001). With distal segments as comparator, the OR for ≥50% stenosis was approximately 1.6-fold (p<0.001) greater for middle segments, and 1.8-fold (p=0.001) greater for proximal segments. With the RCA as comparator, the OR was approximately 0.7-fold (p = 0.039) smaller for the LCx, and 0.2-fold (p <0.001) smaller for the LM; the OR's for the RCA and LAD were similar. For each unit of natural log of SCS, the OR of ≥50% stenosis was 1.5-fold (p <0.001) greater. The presence of spotty calcifications had an OR for stenosis approximately 2.7-fold (p <0.001) greater than the absence of calcification, wide calcifications approximately 4.3-fold (p <0.001) greater, and diffuse calcifications approximately 9.1-fold (p <0.001) greater than the absence of calcification.

Multivariable analysis (Table 5)

In a GEE model, the OR for coronary stenosis was approximately 1.8-fold greater (p = 0.006) in patients with typical chest pain, 2-fold (p = 0.014) greater in patients with acute coronary syndrome, and 2-fold greater (p <0.001) in patients with prior myocardial infarction. The presence of spotty calcifications had an OR for stenosis approximately 2.3-fold (p <0.001) greater than the

absence of calcification, wide calcifications approximately 2.7-fold (p <0.001) greater, and diffuse calcifications approximately 4.6-fold (p <0.001) greater than the absence of calcification. With distal segments as comparator, each unit of natural log of SCS in middle segments corresponded to an OR approximately 1.2-fold (p <0.001) greater; in proximal segments this corresponded to an OR 1.1-fold greater (p = 0.021). The LM coronary artery had an OR for stenosis approximately 0.2-fold (p = 0.001) smaller than the RCA, whereas the remaining coronary vessels were similar.

Prediction score

Based on the coefficients (multiplied by 100) of the final GEE model (Table 5), a score for the prediction of the probability of ≥50% stenosis in a given segment (*P-score*) was calculated as follows:

P-score = 12*ln(SCS) (if proximal) + 17*ln(SCS) (if middle) + 83 (if spotty) + 99 (if wide) + 153 (if diffuse) + 56 (if typical chest pain) + 69 (if acute coronary syndrome) + 68 (if prior myocardial infarction) -178 (if LM) -362

The probability of ≥50% coronary stenosis increased with the extent (i.e., SCS, morphology) of coronary calcification. This probability was related to the *P-score* through the following equation:

Probability (≥50% stenosis) = 1 / [1 + exp (- *P-score*)]

Training set and test set (Figure 5)

The prediction model showed a good diagnostic performance when validated in the test set. The AUC in the test set was 0.786 (CI: 0.757-0.814). This value was similar to the AUC in the training set that was 0.795 (CI: 0.770-0.819) showing a consistent performance. The Youden's index in the training set gave an optimal probability threshold equal to or greater than 9.2%, which yielded sensitivity and specificity of 0.752 and 0.712, respectively. In the test set, the optimal probability threshold was equal to or greater than 6.8%, which yielded sensitivity and specificity of 0.748 and 0.689, respectively.

Discussion

Summary of findings

The probability of ≥50% diameter stenosis increased with segmental calcium score (SCS), and from the spotty, to the wide, to the diffuse calcification morphology (Figure 4, left column), in keeping with findings by Lau et al. (16) and Kajinami et al. (14). For both SCS and calcification morphology the use of a high-specificity threshold was associated with a much lower sensitivity, and a high-sensitivity threshold was associated with a much lower specificity (Figure 4, right column), implying that SCS and calcification morphology if used *per se* were rather crude predictors of ≥50% stenosis. The compensatory enlargement of atherosclerotic coronary arteries (positive vessel wall remodeling) may explain this finding (17). By combining patient's symptoms, clinical history and lesion location within the coronary tree, the predictive value of SCS and calcification morphology could be improved. **We developed a multivariable prediction model based on segmental calcium score (SCS), calcification morphology, the patient's symptoms and clinical history to predict the probability of ≥50% diameter stenosis in the same coronary segment. The prediction model was tested in a test sample not used for the development of the formula and revealed consistent performance.**

Clinical implications

The total Agatston calcium score is a sensitive predictor of coronary stenosis anywhere in the coronary tree when a low positivity cut-off is used (94% sensitivity with a cut-off of Agatston score greater than 0), but with a poor specificity (47% specificity) (2). On the other hand, if a higher cut-off is chosen, coronary calcium has better specificity at the expense of sensitivity.

There is a weak relationship between intermediate calcium scores (e.g., between 100 and 399) and associated stenosis. CCTA can partly overcome this weakness (18). The interpretation of CCTA however can be challenged by focal bulky calcifications. Bulky calcifications can be expected in 10% of coronary segments in patients with intermediate pre-test likelihood of coronary artery disease, and of these one in four are associated with significant stenoses (19). Bulky calcifications typically lead to overestimation of lesion severity (false positive diagnosis) (19-22)

related to limited spatial resolution of CCTA and the resulting visual impression known as the 'blooming effect'. Whether focal segmental calcifications can help predict the probability of underlying coronary stenosis was the research question addressed by this study.

The formula described here may help estimate the probability of significant stenosis in the context of reading CCTA in a patient with focal bulky calcifications. Whether or not further action should be taken - either ordering a further diagnostic test or initiating aggressive medical therapy - will not depend exclusively on the result of the prediction model, but rather on the global patient assessment. For instance, in a patient with suspected high-risk coronary artery disease (defined as 2-vessel disease involving the LAD, 3-vessel disease or involvement of the LM) further testing and intention to treat may be the first option, as these patients would benefit from revascularization (23, 24). On the other hand, in a patient with low-risk coronary artery disease (e.g. 1-vessel disease involving a non-prognostic vessel) aggressive medical treatment may be the first option.

The diagnostic performance of the prediction model in the test sample (AUC = 0.786) was worse than that of patient-level Agatston calcium score (AUC = 0.851). However, a direct comparison does not make sense because the total Agatston score is predictive of stenosis anywhere in the coronary tree at the patient level, whereas the rationale of this prediction model is at segmental or lesion level, not at the patient level. The prediction model may help in a subset of patients with intermediate total Agatston calcium scores (100-399) and one or two bulky calcified plaques that challenge CCTA interpretation.

Sharp reconstruction kernels partially compensate for the blooming effect, however this comes at the expense of increased image noise. Deconvolution filters require long computational times and have not been validated in clinical practice (25). Dual-energy scan techniques allow the acquisition of separate low- and high-energy images which are then synthesized to cancel high-density structures such as calcifications (26, 27). Compared to the conventional (single-energy) scan technique, these approaches are characterised by roughly double temporal resolution or spatial resolution, hence the added value for coronary artery imaging in patients remains uncertain. The

possibility of obtaining virtual non-contrast images from a single contrast-enhanced CCTA (28) may obviate the need to perform a non-enhanced scan prior to CCTA. Iterative reconstruction algorithms can reduce radiation exposure to patients without decreasing overall image quality in coronary calcium scoring (29) and CCTA (30), however their effect on the diagnostic performance of CCTA in severely calcified coronary arteries has not been firmly established.

Limitations

The Agatston calcium score is not a physical measurement of calcification (11). There was however a very high correlation between the Agatston and the volume/mass scores. SCS does not include non-calcified plaque. The training set and test set included two groups of consecutive patients. Small differences between groups may explain the slightly poorer fitting of the model on the test set compared to the training set. The test set had less patients with typical chest pain and more patients with atypical chest pain. The test set may thus represent a slightly more challenging patient group. The reported results are therefore a conservative estimate of the prediction model's performance. Further research may be warranted to define in which patient population the analysis of SCS additional to CCTA may be most beneficial to improve diagnostic performance.

Future developments

The semi-automated quantification of coronary plaque burden and components (calcified and non-calcified) may represent a more accurate approach for the characterisation of coronary artery plaques (31-34). These methods however require time-intensive manual input, as opposed to the quick method described here. The feasibility of stress myocardial CT perfusion imaging has been demonstrated recently (35-40) as capable of adding functional information on the haemodynamic significance of coronary stenoses. However, CT perfusion imaging requires additional patient radiation exposure, contrast administration and the administration of a pharmacological stress agent. The possibility of a CT-derived fractional flow reserve measurement based on computational fluid dynamics modelling, albeit computationally difficult and time-consuming, has also been shown with very promising results (41). The utility of computational FFR in heavily calcified coronary vessels (Agatston score >400), however, remains uncertain.

Conflict of Interest

None declared.

References

1. Bielak LF, Rumberger JA, Sheedy PF, 2nd, et al. Probabilistic model for prediction of angiographically defined obstructive coronary artery disease using electron beam computed tomography calcium score strata. Circulation. 2000;102(4):380-5.

2. Breen JF, Sheedy PF, 2nd, Schwartz RS, et al. Coronary artery calcification detected with ultrafast CT as an indication of coronary artery disease. Radiology. 1992;185(2):435-9.

3. Budoff MJ, Diamond GA, Raggi P, et al. Continuous probabilistic prediction of angiographically significant coronary artery disease using electron beam tomography. Circulation. 2002;105(15):1791-6.

4. Haberl R, Becker A, Leber A, et al. Correlation of coronary calcification and angiographically documented stenoses in patients with suspected coronary artery disease: results of 1,764 patients. J Am Coll Cardiol. 2001;37(2):451-7.

5. Meijboom WB, van Mieghem CA, Mollet NR, et al. 64-slice computed tomography coronary angiography in patients with high, intermediate, or low pretest probability of significant coronary artery disease. J Am Coll Cardiol. 2007;50(15):1469-75.

6. Meijboom WB, Weustink AC, Pugliese F, et al. Comparison of diagnostic accuracy of 64-slice computed tomography coronary angiography in women versus men with angina pectoris. Am J Cardiol. 2007;100(10):1532-7.

7. Mollet NR, Cademartiri F, van Mieghem CA, et al. High-resolution spiral computed tomography coronary angiography in patients referred for diagnostic conventional coronary angiography. Circulation. 2005;112(15):2318-23.

8. Hausleiter J, Meyer T, Hermann F, et al. Estimated radiation dose associated with cardiac CT angiography. Jama. 2009;301(5):500-7.

9. Austen WG, Edwards JE, Frye RL, et al. A reporting system on patients evaluated for coronary artery disease. Report of the Ad Hoc Committee for Grading of Coronary Artery Disease, Council on Cardiovascular Surgery, American Heart Association. Circulation. 1975;51(4 Suppl):5-40.

10. Mark DB, Berman DS, Budoff MJ, et al. ACCF/ACR/AHA/NASCI/SAIP/SCAI/SCCT 2010 expert consensus document on coronary computed tomographic angiography: a report of the American College of Cardiology Foundation Task Force on Expert Consensus Documents. J Am Coll Cardiol. 2010;55(23):2663-99.

11. Agatston AS, Janowitz WR, Hildner FJ, et al. Quantification of coronary artery calcium using ultrafast computed tomography. J Am Coll Cardiol. 1990;15(4):827-32.

12. Callister TQ, Cooil B, Raya SP, et al. Coronary artery disease: improved reproducibility of calcium scoring with an electron-beam CT volumetric method. Radiology. 1998;208(3):807-14.

13. McCollough CH, Ulzheimer S, Halliburton SS, et al. Coronary artery calcium: a multi-institutional, multimanufacturer international standard for quantification at cardiac CT. Radiology. 2007;243(2):527-38.

14. Kajinami K, Seki H, Takekoshi N, Mabuchi H. Coronary calcification and coronary atherosclerosis: site by site comparative morphologic study of electron beam computed tomography and coronary angiography. J Am Coll Cardiol. 1997;29(7):1549-56.

15. Pugliese F, Mollet NR, Hunink MG, et al. Diagnostic performance of coronary CT angiography by using different generations of multisection scanners: single-center experience. Radiology. 2008;246(2):384-93.

16. Lau GT, Ridley LJ, Schieb MC, et al. Coronary artery stenoses: detection with calcium scoring, CT angiography, and both methods combined. Radiology. 2005;235(2):415-22.

17. Glagov S, Weisenberg E, Zarins CK, et al. Compensatory enlargement of human atherosclerotic coronary arteries. N Engl J Med. 1987;316(22):1371-5.

18. Hadamitzky M, Distler R, Meyer T, et al. Prognostic value of coronary computed tomographic angiography in comparison with calcium scoring and clinical risk scores. Circ Cardiovasc Imaging. 2011;4(1):16-23.

19. Meijboom WB, Meijs MF, Schuijf JD, et al. Diagnostic accuracy of 64-slice computed tomography coronary angiography: a prospective, multicenter, multivendor study. J Am Coll Cardiol. 2008;52(25):2135-44.

20. Abdulla J, Pedersen KS, Budoff M, Kofoed KF. Influence of coronary calcification on the diagnostic accuracy of 64-slice computed tomography coronary angiography: a systematic review and meta-analysis. Int J Cardiovasc Imaging. 2012;28(4):943-53.

21. Alkadhi H, Scheffel H, Desbiolles L, et al. Dual-source computed tomography coronary angiography: influence of obesity, calcium load, and heart rate on diagnostic accuracy. Eur Heart J. 2008;29(6):766-76.

22. Yan RT, Miller JM, Rochitte CE, et al. Predictors of inaccurate coronary arterial stenosis assessment by CT angiography. JACC. Cardiovascular imaging. 2013;6(9):963-72.

23. de Feyter PJ, Nieman K. CCTA to guide revascularization for high-risk CAD: a 'cliff hanger'. Eur Heart J. 2012;33(24):3011-3.

24. Min JK, Berman DS, Dunning A, et al. All-cause mortality benefit of coronary revascularization vs. medical therapy in patients without known coronary artery disease undergoing coronary computed tomographic angiography: results from CONFIRM (COronary CT Angiography EvaluatioN For Clinical Outcomes: An InteRnational Multicenter Registry). Eur Heart J. 2012;33(24):3088-97.

25. Rollano-Hijarrubia E, Niessen W, Weinans H, et al. Histogram-based selective deblurring to improve computed tomography imaging of calcifications. Invest Radiol. 2007;42(1):8-22.

26. Johnson TR, Krauss B, Sedlmair M, et al. Material differentiation by dual energy CT: initial experience. Eur Radiol. 2007;17(6):1510-7.

27. Schwarz F, Nance JW, Jr., Ruzsics B, et al. Quantification of coronary artery calcium on the basis of dual-energy coronary CT angiography. Radiology. 2012;264(3):700-7.

28. Bischoff B, Kantert C, Meyer T, et al. Cardiovascular risk assessment based on the quantification of coronary calcium in contrast-enhanced coronary computed tomography angiography. Eur Heart J Cardiovasc Imaging. 2012;13(6):468-75.

29. Schindler A, Vliegenthart R, Schoepf UJ, et al. Iterative image reconstruction techniques for CT coronary artery calcium quantification: comparison with traditional filtered back projection in vitro and in vivo. Radiology. 2014;270(2):387-93.

30. Gosling O, Loader R, Venables P, et al. A comparison of radiation doses between state-of-the-art multislice CT coronary angiography with iterative reconstruction, multislice CT coronary angiography with standard filtered back-projection and invasive diagnostic coronary angiography. Heart. 2010;96(12):922-6.

31. Dey D, Schepis T, Marwan M, et al. Automated three-dimensional quantification of noncalcified coronary plaque from coronary CT angiography: comparison with intravascular US. Radiology. 2010;257(2):516-22.

32. Leber AW, Becker A, Knez A, et al. Accuracy of 64-slice computed tomography to classify and quantify plaque volumes in the proximal coronary system: a comparative study using intravascular ultrasound. J Am Coll Cardiol. 2006;47(3):672-7.

33. Schepis T, Marwan M, Pflederer T, et al. Quantification of non-calcified coronary atherosclerotic plaques with dual-source computed tomography: comparison with intravascular ultrasound. Heart. 2010;96(8):610-5.

34. Sun J, Zhang Z, Lu B, et al. Identification and quantification of coronary atherosclerotic plaques: a comparison of 64-MDCT and intravascular ultrasound. AJR Am J Roentgenol. 2008;190(3):748-54.

35. Bamberg F, Becker A, Schwarz F, et al. Detection of hemodynamically significant coronary artery stenosis: incremental diagnostic value of dynamic CT-based myocardial perfusion imaging. Radiology. 2011;260(3):689-98.

36. Bamberg F, Hinkel R, Schwarz F, et al. Accuracy of dynamic computed tomography adenosine stress myocardial perfusion imaging in estimating myocardial blood flow at various degrees of coronary artery stenosis using a porcine animal model. Invest Radiol. 2012;47(1):71-7.

37. Ho KT, Chua KC, Klotz E, Panknin C. Stress and rest dynamic myocardial perfusion imaging by evaluation of complete time-attenuation curves with dual-source CT. JACC. Cardiovascular imaging. 2010;3(8):811-20.

38. Rochitte CE, George RT, Chen MY, et al. Computed tomography angiography and perfusion to assess coronary artery stenosis causing perfusion defects by single photon emission computed tomography: the CORE320 study. Eur Heart J. 2014;35(17):1120-30.

39. Rossi A, Dharampal A, Wragg A, et al. Diagnostic performance of hyperaemic myocardial blood flow index obtained by dynamic computed tomography: does it predict functionally significant coronary lesions? Eur Heart J Cardiovasc Imaging. 2014;15(1):85-94.

40. Rossi A, Uitterdijk A, Dijkshoorn M, et al. Quantification of myocardial blood flow by adenosine-stress CT perfusion imaging in pigs during various degrees of stenosis correlates well with coronary artery blood flow and fractional flow reserve. Eur Heart J Cardiovasc Imaging. 2013;14(4):331-8.

41. Norgaard BL, Leipsic J, Gaur S, et al. Diagnostic performance of noninvasive fractional flow reserve derived from coronary computed tomography angiography in suspected coronary artery disease: the NXT trial (Analysis of Coronary Blood Flow Using CT Angiography: Next Steps). J Am Coll Cardiol. 2014;63(12):1145-55.

42. Budoff MJ, Achenbach S, Blumenthal RS, et al. Assessment of coronary artery disease by cardiac computed tomography: a scientific statement from the American Heart Association Committee on Cardiovascular Imaging and Intervention, Council on Cardiovascular Radiology and Intervention, and Committee on Cardiac Imaging, Council on Clinical Cardiology. Circulation. 2006;114(16):1761-91.

Tables

Table 1. Classification of calcification morphology on non-enhanced CT images. Modified from Kajinami et al. (14).

Calcification morphology	Lesion width [a]	Lesion length [b]
Diffuse	≥2/3 of coronary diameter	≥3/2 of coronary diameter
Wide	≥2/3 of coronary diameter or <2/3 of coronary diameter	<3/2 of coronary diameter ≥3/2 of coronary diameter
Spotty	<2/3 of coronary diameter	<3/2 of coronary diameter
None	Undetectable	Undetectable

[a] Extent of calcification perpendicular to the longitudinal direction of the vessel
[b] Extent of lesion in the longitudinal direction of the vessel

Table 2. Baseline characteristics.

Characteristic		Training sample	Test sample	p-value [e]
No. of patients		201	201	-
Age				
Mean age (sd) [a] (years)		59 (12)	60 (10)	0.52 [f]
Age range		21-87	35-80	-
Age groups: no. (%)		-	-	0.81
	≤50	38/201 (19%)	33/201 (17%)	-
	51-60	79/201 (39%)	80/201 (40%)	-
	61-70	50/201 (25%)	57/201 (28%)	-
	>70	34/201 (17%)	31/201 (15%)	-
Men / Women: no. (%)		142 (71%) / 59 (29%)	137 (68%) / 64 (32%)	0.59
Patient clinical presentation: no. (%)				
Typical chest pain [b]		97/201 (48%)	57/201 (28%)	<0.001
Atypical chest pain [c]		71/201 (35%)	76/201 (38%)	0.61
Acute coronary syndrome [d]		33/201 (17%)	68/201 (34%)	<0.001
Cardiovascular risk factors: no. (%)				
Obesity (Body Mass Index ≥30 Kg/m^2)		48/201 (24%)	50/201 (25%)	0.84
Smoking (current or past)		63/201 (31%)	66/201 (33%)	0.75
Hypertension (blood pressure ≥140/90 mmHg, or on anti-hypertension medication)		106/201 (53%)	110/201 (55%)	0.69
Dyslipidemia (serum cholesterol >200 mg/dL or 5.18 mmol/L)		136/201 (68%)	100/201 (50%)	<0.001
Diabetes mellitus (plasma glucose ≥126 mg/dL or 7.0 mmol/L)		25/201 (12%)	26/201 (13%)	0.88
Family history (presence of CAD in a first-degree female [<65 years] or male [<55 years] relative)		90/201 (45%)	106/201 (53%)	0.11
Prior myocardial infarction		43/201 (21%)	21/201 (11%)	0.003
Medication before MSCT and heart rate				
Beta-blockers: no. (%)		142/201 (71%)	135/201 (67%)	0.11
Mean heart rate during scan (sd) [a] (beats/min.)		58 (11)	60 (8)	0.77
Total calcium score (Agatston; patient level)				
Range		0-3839	0-3394	-
Mean (sd) [a]		450.37 (661.23)	346.60 (492.02)	0.70 [f]
Median (IQ) [g]		198.10 (10.65 - 557.40)	214.70 (14.70 - 443.80)	1.00 [h]
Calcium score groups: no. (%)		-	-	0.79
	0-10	50/201 (25%)	47/201 (23%)	-
	11-100	32/201 (16%)	32/201 (16%)	-
	101-400	59/201 (29%)	68/201 (34%)	-
	>400	60/201 (30%)	54/201 (27%)	-

[a] standard deviation; [b] retrosternal pain occurring with exercise, relieved by rest and by administration of nitrates; [c] any 2 or 1 features of typical chest pain; [d] unstable angina or non-ST elevation myocardial infarction; [e] Chi squared test unless otherwise specified; [f] Mann-Whitney U test; [g] interquartile range; [h] independent samples median test.

Table 3. Frequency of significant stenoses in relation to SCS ranges and morphology (in men and women according to age).

	SCS					Calcification morphology				
	0-10	**11-50**	**51-100**	**>100**	**p-value***	**none**	**spotty**	**wide**	**diffuse**	**p-value***
Men										
≤50	16/384 (4.2%)	2/17 (11.8%)	0/2 (0%)	1/4 (25%)	0.114	11/328 (3.4%)	5/58 (8.6%)	1/13 (7.7%)	2/8 (25%)	**0.012**
51-60	43/623 (6.9%)	20/11 (18%)	12/63 (19%)	25/71 (35.2%)	**<0.001**	20/495 (4%)	20/140 (14.3%)	20/113 (17.7%)	40/120 (33.3%)	**<0.001**
61-70	13/260 (5%)	6/59 (10.2%)	9/35 (25.7%)	26/89 (29.2%)	**<0.001**	7/198 (3.5%)	5/63 (7.9%)	14/70 (20%)	28/112 (25%)	**<0.001**
>70	20/162 (12.3%)	8/39 (20.5%)	4/36 (11.1%)	15/49 (30.6%)	**0.016**	12/117 (10.3%)	7/48 (14.6%)	8/57 (14%)	20/64 (31.3%)	**0.003**
Women										
≤50	4/139 (2.9%)	0/6 (0%)	0/2 (0%)	value not observed	0.888	3/130 (2.3%)	1/13 (7.7%)	0/3 (0%)	0/1 (0%)	0.703
51-60	3/234 (1.3%)	0/10 (0%)	2/99 (22.2%)	3/4 (75%)	**<0.001**	3/211 (1.4%)	0/24 (0%)	2/11 (18.2%)	3/11 (27.3%)	**<0.001**
61-70	16/209 (7.7%)	7/39 (17.9%)	1/14 (7.1%)	5/14 (35.7%)	**0.003**	8/170 (4.7%)	6/48 (12.5%)	5/31 (16.1%)	10/27 (37%)	**<0.001**
>70	7/114 (6.1%)	4/35 (11.4%)	2/8 (25%)	8/24 (33.3%)	**0.001**	4/86 (4.7%)	5/37 (13.5%)	4/27 (14.8%)	8/31 (25.8%)	**0.014**

* Chi squared test. Significant p-values are **bolded.**

Table 4. Univariable logistic regression models for the prediction of angiographically proven significant coronary stenosis.

Characteristic	Odds Ratio (95% CI)	p-value*
Age	1.032 (1.015-1.0494)	**<0.001**
Gender (male)	1.629 (1.086-2.445)	**0.018**
Typical chest pain	1.694 (1.178-2.438)	**0.005**
Atypical chest pain	0.340 (0.214-0.538)	**<0.001**
Acute coronary syndrome	1.625 (1.068-2.472)	**0.023**
Obesity	0.986 (0.679-1.432)	0.941
Smoking	1.069 (0.755-1.513)	0.708
Hypertension	1.098 (0.763-1.579)	0.615
Dyslipidemia	2.606 (1.523-4.459)	**<0.001**
Diabetes	0.819 (0.513-1.307)	0.402
Family history of CAD	0.781 (0.550-1.108)	0.166
Prior myocardial infarction	2.537 (1.776-3.623)	**<0.001**
Segment location**		
Distal and side branches	odds ratio comparator	
Middle	2.545 (1.913-3.386)	**<0.001**
Proximal	1.777 (1.272-2.483)	**0.001**
Vessel		
RCA	odds ratio comparator	
LAD	0.995 (0.718-1.379)	0.976
LCx	0.722 (0.529-0.984)	**0.039**
LM	0.150 (0.054-0.416)	**<0.001**
SCS (ln)	1.500 (1.399-1.604)	**<0.001**
Calcification morphology		
Spotty	2.732 (1.898-3.934)	**<0.001**
Wide	4.269 (2.836-6.427)	**<0.001**
Diffuse	9.144 (6.297-13.277)	**<0.001**

*Significant p-values are **bolded.**
** Proximal segments included segments 1, 5, 6, and 11. Middle segments included segments 2, 3, 7, and 13. Distal and side branches included segments 4a, 4b, 8, 9, 10, 12, 14, 15, and 16 (9, 15).

Table 5. GEE logistic regression (final) model for the prediction of angiographically proven significant coronary stenosis.

Model*	Odds Ratio (95% CI)	p-value**	Coefficient
Clinical presentation			
Typical chest pain	1.755 (1.175-2.622)	**0.006**	0.562
Acute coronary syndrome	1.989 (1.151-3.439)	**0.014**	0.688
Risk factors			
Prior myocardial infarction	1.982 (1.397-2.812)	**<0.001**	0.684
Vessel			
LM	0.169 (0.059-0.482)	**0.001**	-1.776
Calcification morphology			
Spotty	2.303 (1.567-3.384)	**<0.001**	0.834
Wide	2.690 (1.698-4.260)	**<0.001**	0.989
Diffuse	4.614 (2.842-7.491)	**<0.001**	1.529
SCS (ln)			
If middle segment	1.189 (1.084-1.304)	**<0.001**	0.173
If proximal segment	1.125 (1.018-1.242)	**0.021**	0.117

* The model Wald chi-square was 226.32 (p <0.001).
** Only variables that retained significant p-values in the multivariable model are reported here. Age, gender, atypical chest pain, dyslipidemia and LCx vessel location had significant p-values at univariable analysis, but not at multivariable analysis.

Figure Legends

Figure 1. Method for the measurement of segmental calcium score (SCS).
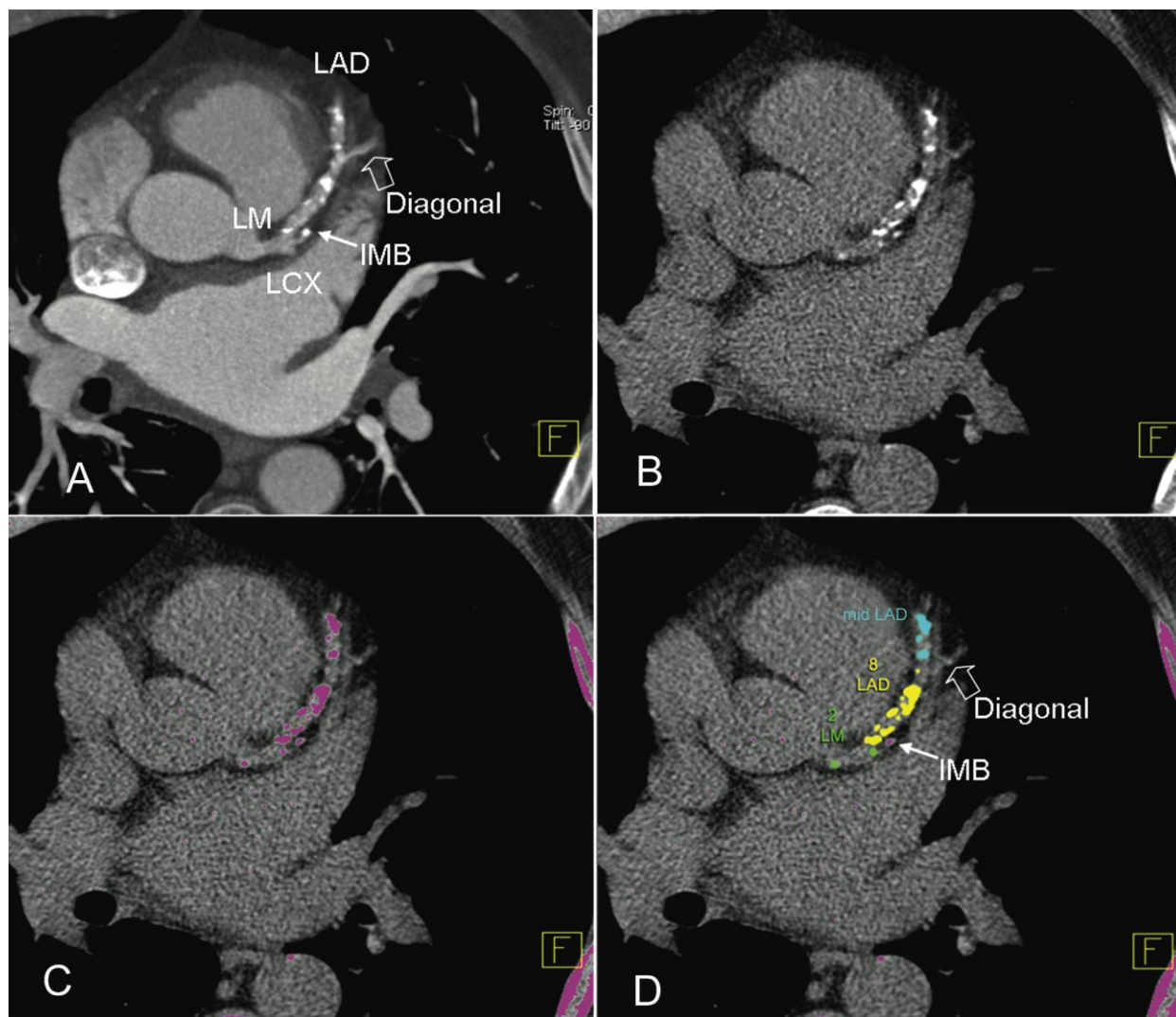

Figure 1. Method for the measurement of segmental calcium score (SCS).

In order to obtain a consistent anatomic classification of the coronary tree into segments, contrast-enhanced CCTA axial images (A) were available to the observer. The CCTA images were scrolled using a viewing application (syngo Viewing, Siemens, Erlangen, Germany). Availability of CCTA ensured the visualization of the origin of smaller side branches, especially when they were not calcified. These side branches might have remained undetected on the non-enhanced images (B, C). The visualization of the diagonal branches allowed the classification into segments of the left anterior descending coronary artery (LAD); the origin of marginal obtuse branches allowed the classification into segments of the left circumflex artery (LCx), and the origin of acute marginal branches allowed the classification into segments of the right coronary artery (RCA). CCTA was used exclusively for the correct anatomical

classification of coronary segments and not for SCS measurement or estimation of stenosis severity. SCS was measured on non-enhanced images (42). Individual coronary segments were labelled according to a standard 17-segment anatomical (D).

LM = left main artery; LAD = left anterior descending artery; LCx = left circumflex; IMB = intermediate branch.

Figure 2. Method for separation of connected calcifications in a slice.

Figure 2. Method for separation of connected calcifications in a slice.

To assign calcifications to the corresponding individual coronary artery segment, there needed to be separation of connected lesions in a slice (A, B). To achieve this, calcifications were edited manually (C) and split (D) using the '3D Edit' function (C, insert and arrow) of the software (syngo Calcium Scoring).

LAD = left anterior descending artery; LCx = left circumflex.

Figure 3. Classification of calcification morphology.
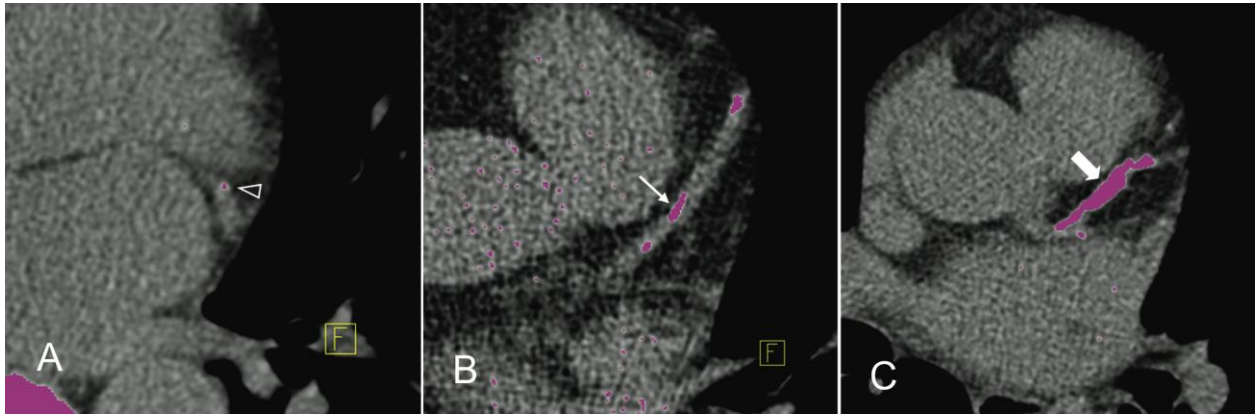
Figure 3. Classification of calcification morphology.

We applied a method validated by Kajinami et al. (14) for the classification of calcification morphology. Calcification morphology was classified visually as spotty (A, arrowhead), wide (B, arrow) and diffuse (C, gross arrow) based on the width and length of the calcification in relation to the coronary segment diameter (full description in Table 1).

Figure 4. Segmental calcium score (SCS) and calcification morphology: frequency of associated significant stenoses (left column) and ROC curves (right column).
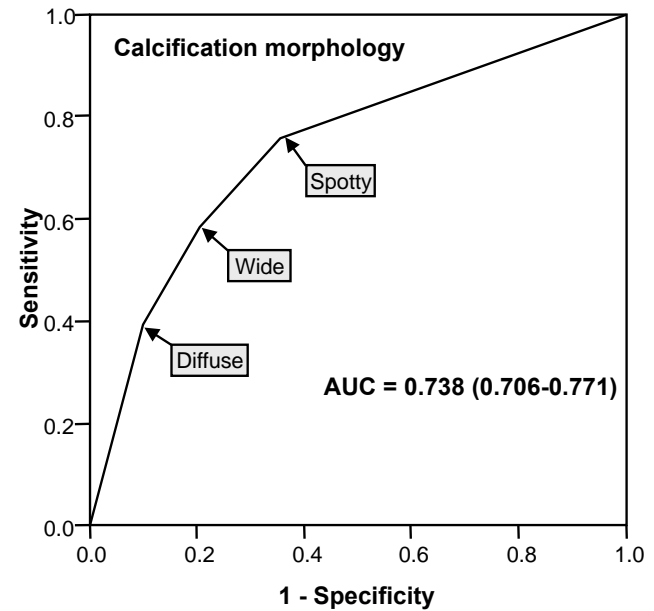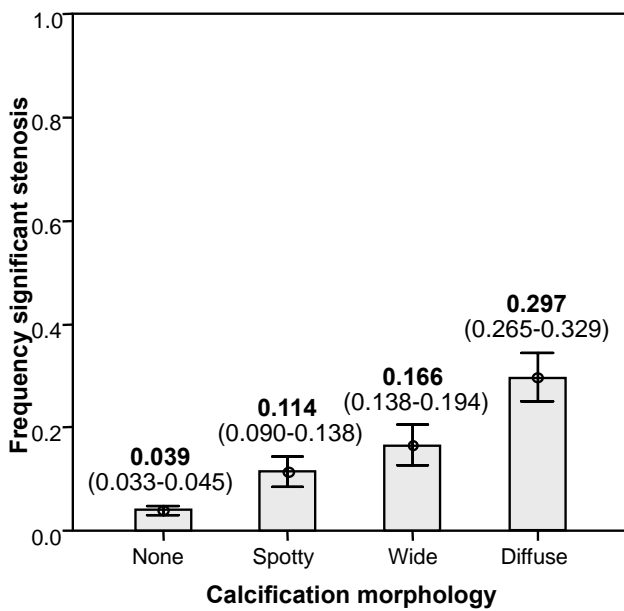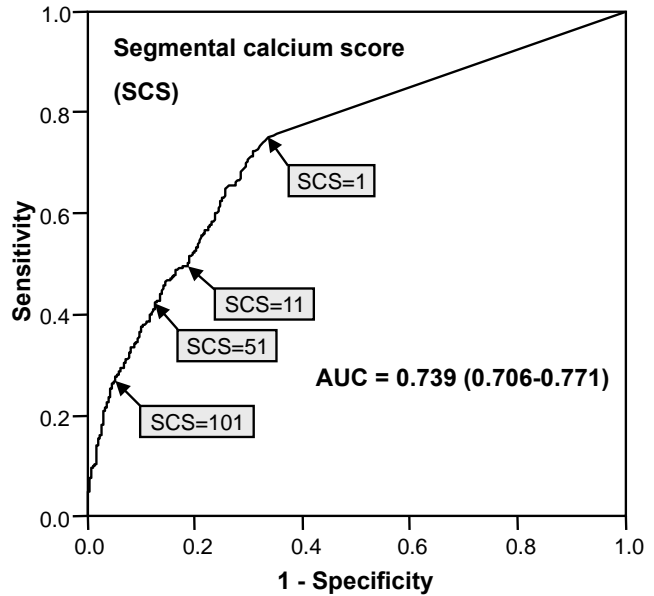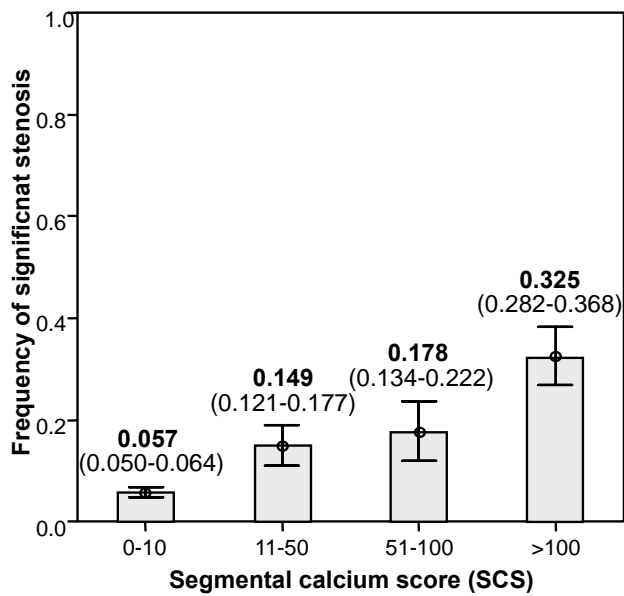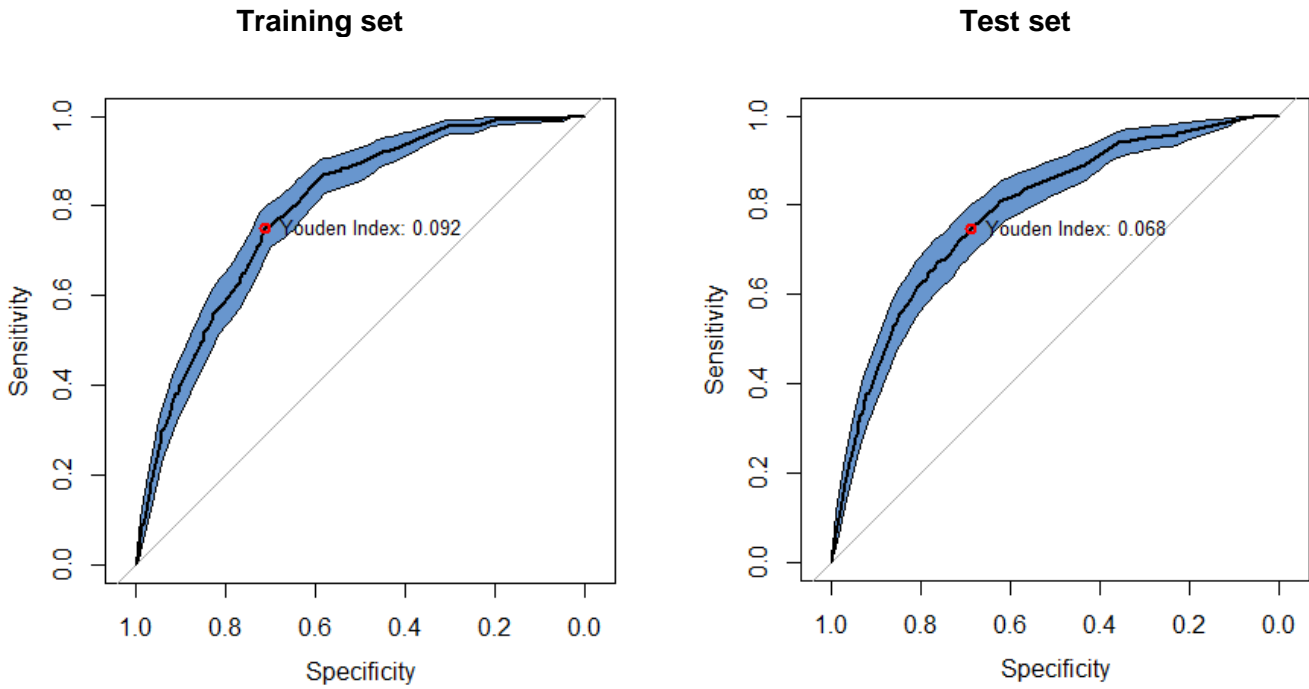

Figure 4. Segmental calcium score (SCS) and calcification morphology: frequency of associated significant stenoses (left column) and ROC curves (right column).

The frequency of coronary stenosis (left column) increased proportionally with increasing SCS. The frequency of stenosis also increased from spotty, to wide, to diffuse morphology. The diagnostic performances of SCS and morphology in the detection of ≥50% stenosis (right column) were similar. Arrows and labels indicate different calcification thresholds for positivity (i.e., ≥50% coronary artery stenosis).
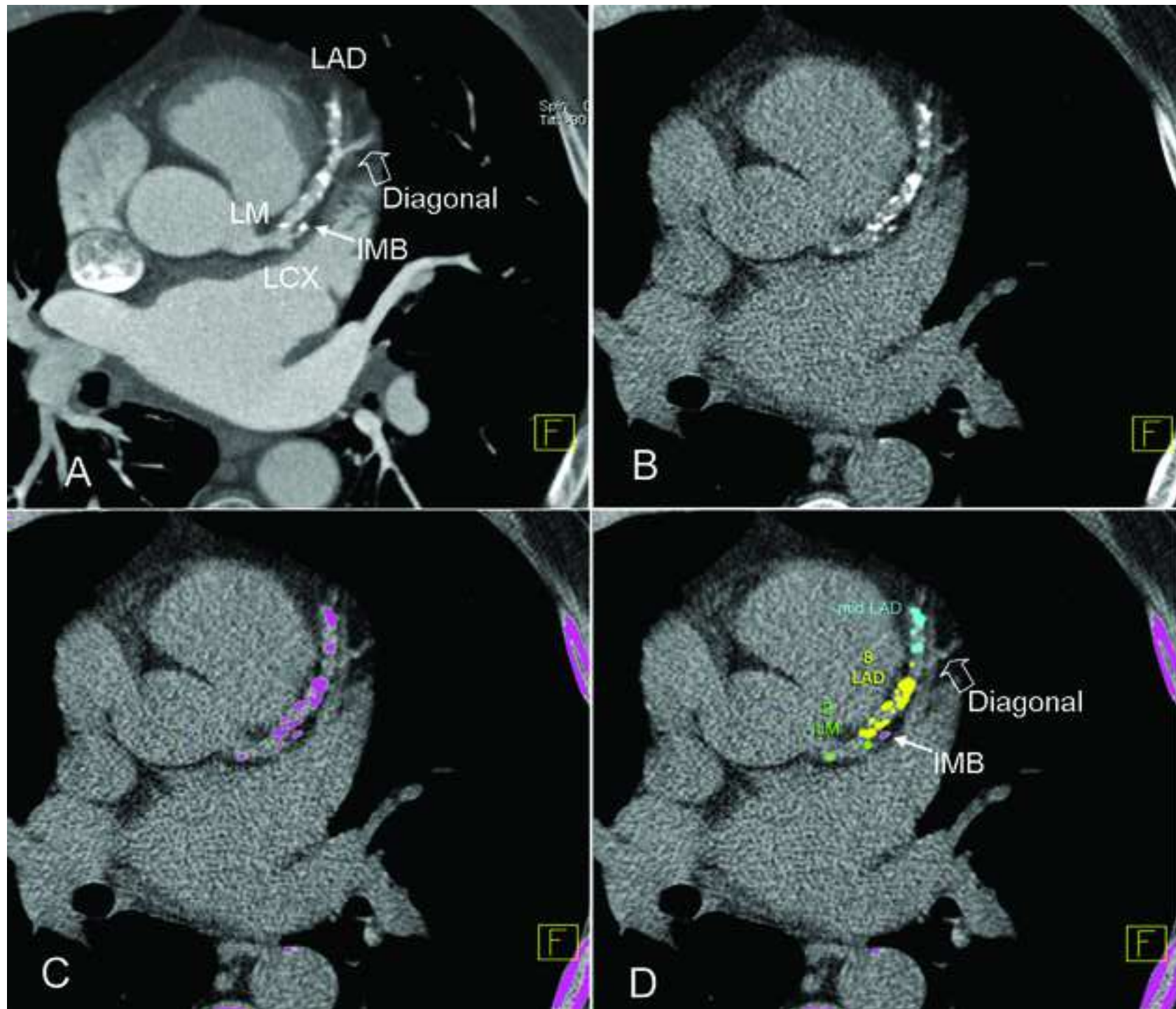
Figure 5. Performance of the multivariable model (ROC curves) in the training set and test set

Figure 5. Performance of the multivariable model (ROC curves) in the training set and test set

The Youden's index in the training set gave an optimal probability threshold equal to or greater than 9.2%, which yielded sensitivity and specificity of 0.752 and 0.712, respectively. In the test set, the optimal probability threshold was equal to or greater than 6.8%, which yielded sensitivity and specificity of 0.748 and 0.689, respectively.

Figure_2
Click here to download Figure: Figure_2.tif

Figure_4
Click here to download Figure: Figure_4.tiff

Upper left panel — Frequency of significicnat stenosis vs Segmental calcium score (SCS):
- 0-10: 0.057 (0.050-0.064)
- 11-50: 0.149 (0.121-0.177)
- 51-100: 0.178 (0.134-0.222)
- >100: 0.325 (0.282-0.368)

Upper right panel — Segmental calcium score (SCS); Sensitivity vs 1 - Specificity:
- SCS=1
- SCS=11
- SCS=51
- SCS=101
- AUC = 0.739 (0.706-0.771)

Lower left panel — Frequency significant stenosis vs Calcification morphology:
- None: 0.039 (0.033-0.045)
- Spotty: 0.114 (0.090-0.138)
- Wide: 0.166 (0.138-0.194)
- Diffuse: 0.297 (0.265-0.329)

Lower right panel — Calcification morphology; Sensitivity vs 1 - Specificity:
- Spotty
- Wide
- Diffuse
- AUC = 0.738 (0.706-0.771)

Computed tomography segmental calcium score (SCS) to predict stenosis severity of calcified coronary lesions

Francesca Pugliese, MD PhD (1)

MG Myriam Hunink, MD PhD (2,3)

Willem B Meijboom, MD PhD (4)

Katarzyna Gruszczynsnka, MD PhD (5)

Marco Rengo, MD (6)

Lu Zou, PhD (7)

Ian Baron, MD (5)

Marcel L Dijkshoorn, MSc RT (2)

Gabriel P Krestin, MD PhD (2)

Pim J de Feyter, MD PhD (2,4)

(1) Centre for Advanced Cardiovascular Imaging, NIHR Cardiovascular Biomedical Research Unit at Barts, William Harvey Research Institute, Barts and The London School of Medicine and Dentistry, Queen Mary University of London (United Kingdom)
(2) Department of Radiology, Erasmus MC University Medical Centre Rotterdam (the Netherlands)
(3) Harvard School of Public Health, Harvard University, Boston (United States)
(4) Department of Cardiology, Erasmus MC University Medical Centre Rotterdam (the Netherlands)
(5) Medical University of Silesia, Katowice (Poland)
(6) University of Rome La Sapienza, Polo Pontino (Italy)
(7) Experimental Medicine and Rheumatology, William Harvey Research Institute, Barts and The London School of Medicine and Dentistry, Queen Mary University of London (United Kingdom)

Address for correspondence:

Dr Francesca Pugliese, MD PhD FESC

Centre for Advanced Cardiovascular Imaging & Cardiac Imaging Department

2nd floor Barts Heart Centre, St Bartholomew's hospital

West Smithfield

London EC1A 7BE (United Kingdom)

Phone: +44 20 7882 6906

Email address: f.pugliese@qmul.ac.uk

✍ Springer

Disclosure of potential conflicts of interest

Authors must disclose all relationships or interests that could have direct or potential influence or impart bias on the work. Although an author may not feel there is any conflict, disclosure of all relationships and interests provides a more complete and transparent process, leading to an accurate and objective assessment of the work. Awareness of a real or perceived conflicts of interest is a perspective to which the readers are entitled. This is not meant to imply that a financial relationship with an organization that sponsored the research or compensation received for consultancy work is inappropriate. For examples of potential conflicts of interests *that are directly or indirectly related to the research* please visit:

springer.com/gp/authors-editors/journal-author/journal-author-helpdesk/before-you-start

International Journal of Cardiovascular Imaging
Corresponding authors of papers submitted to _____
(name of journal) must complete this form and disclose any real or perceived conflict of interest. The corresponding author signs <u>on behalf of all authors.</u>

The corresponding author will include a statement in the text of the manuscript in a separate section before the reference list, that reflects what is recorded in the potential conflict of interest disclosure form. Please note that you cannot save the form once completed. Kindly print upon completion, sign, and scan to keep a copy for your files.

The corresponding author should be prepared to send the potential conflict of interest disclosure form if requested during peer review or after publication on behalf of all authors (if applicable).

☑   We have no potential conflict of interest.

Category of disclosure	Description of Interest/Arrangement

omputed tomography segmental calcium score (SCS) to predict stenosis severity of calcified
Article title _____

Manuscript No. (if you know it) _____

Francesca Pugliese
Corresponding author name _____

Herewith I confirm, on behalf of all authors, that the information provided is accurate.

24 March 2015
Author signature _____Date_____

The International Journal of CARDIOVASCULAR IMAGING
Authorship and Disclosure Form

🐎 **Springer**

Computed tomography segmental calcium score (SCS) to predict stenosis severity of calcified coronary lesions

MANUSCRIPT ID NUMBER

Author's signature

Katarzyna Gruszczynska _31.3.2015_
Printed name and date

Author's signature

Jan Baron _31.3.2015_
Printed name and date

Author's signature

Printed name and date

Author's signature

Printed name and date

Author's signature

Printed name and date

Author's signature

Printed name and date

Author's signature

Printed name and date

Author's signature

Printed name and date

Page 2 of 3- (signatures and dates required on page 2)

The International Journal of CARDIOVASCULAR IMAGING
Authorship and Disclosure Form

🐴 Springer

Computed tomography segmental calcium score (SCS) to predict stenosis severity of calcified coronary lesions

_____
MANUSCRIPT ID NUMBER

_____
Author's signature

Gabriel P Krestin____30.3.2015____
Printed name and date

_____
Author's signature

MG Myriam Hunink___30 / 03 / 2015
Printed name and date

31.3.2015
_____
Author's signature

Pim de Feyter_____
Printed name and date

30 /03/2015
_____
Author's signature

Bob W Meijboom_____
Printed name and date

_____
Author's signature

Marcel Dijkshoorn_____
Printed name and date

_____
Author's signature

_____
Printed name and date

_____
Author's signature

_____
Printed name and date

_____
Author's signature

_____
Printed name and date

Page 2 of 3- (signatures and dates required on page 2)

The International Journal of CARDIOVASCULAR IMAGING
Authorship and Disclosure Form

Springer

Computed tomography segmental calcium score (SCS) to predict stenosis severity of calcified coronary lesions

_____

MANUSCRIPT ID NUMBER

_____
Author's signature

Francesca Pugliese___31/03/15___
Printed name and date

_____
Author's signature

Lu Zou___31.03.2015___
Printed name and date

_____
Author's signature

Marco Rengo___30 March 15___
Printed name and date

_____
Author's signature

_____
Printed name and date

_____
Author's signature

_____
Printed name and date

_____
Author's signature

_____
Printed name and date

_____
Author's signature

_____
Printed name and date

_____
Author's signature

_____
Printed name and date

Page 2 of 3- (signatures and dates required on page 2)

The International Journal of CARDIOVASCULAR IMAGING Authorship and Disclosure Form

🐴 Springer

MANUSCRIPT ID NUMBER

CT SEGMENTAL CALCIUM SCORE (SCS) TO PREDICT STENOSIS SEVERITY OF CALCIFIED CORONARY LESIONS

Author's signature

Printed name and date

Author's signature

MARCEL L. DIJKSHOORN 31.3.15
Printed name and date

M. Dijkshoorn
Author's signature

Printed name and date

Author's signature

Printed name and date

Author's signature

Printed name and date

Author's signature

Printed name and date

Author's signature

Printed name and date

Page 2 of 3- (signatures and dates required on page 2)